Cooperating not-trushting robots

Ing. Filip Kovář

Supervisor: Prof. Ing. Michael Valášek, DrSc.

Abstract
This paper deals with the simulation of cooperating robots. The tested models are two planar two-arm robots. The connecting element between robots is realized as a spring and a damper. The control system is implemented by two cascade control loops. One loop monitors the position of the motor and the other monitors the position of the arm. There has been found improvement of the dynamic stiffness and accuracy.

Index Terms
Cooperation of robots, redundant kinematics, parallel kinematics, thrusting of redundant systems, design of dynamic systems, control of dynamic systems, cascade control, moment compensation.

1. Introduction

In the last twenty years we can observe rapid development in the field of machine tools mainly because of the increasing performance and reliability of measuring and control elements. For machining mechanisms, the development is first of all focused on dynamics increase while improving rigidity and machinery precision too. The traditional machines with linear kinematics can meet these three requirements only to a certain level. That is how the opportunity for redundantly driven parallel kinematics was created. Redundantly driven system is the one that contains more actuators than the number of degrees of freedom. In parallel kinematics end gripper or platform holds more arms.
The advantage of system with parallel kinematics is its high structural rigidity and positioning accuracy. Generally we can also observe simpler frame parts with low weight. Among the disadvantages we can especially mention high demands on the control and scanning of machine kinematics.

Picture 1 *- SlidingStar*

Nowadays, there are machines proving that the development of mechanisms with parallel kinematics really brings results. A good example is the new mechanism of machine tools

Trijoint 900H [4] and SlidingStar [5] (on the *Picture 1*), they arose from the Faculty of Mechanical Engineering CTU in Prague. There was a double to quadruple increase in dynamics, rigidity and accuracy compared to conventional machine tools.
Following the successful achievement of improved parameters we can talk about idea of multi-axis machines. An example of such a robot is shown in the *Picture 2* [6]. As a consequence of the connection of robot endpoint and traditional linear structure, it may lead to the machine tool with parallel kinematics, which would have very good availability in the workspace.

***Picture 2**- Robot with linear structure*

2. Mathematical model

For testing of the basic properties we have chosen two-arm planar robot. First, we built a simulation model of a single robot. On the Picture 3 there is a scheme of the robot.

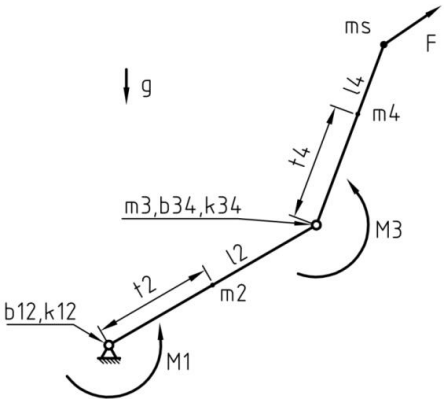

***Picture 3**- Robot scheme*

The constants of the model correspond to the expected real machine. We have also added to the model the submissiveness of drives and then we proposed cascade control. In the last step of compiling the model, we joined two robots using model of spring and damper. We chose constants with respect to the expected connection through spindle.

2.1 Drive submissiveness

The principle of submissiveness is shown on the *Picture 4* on left side. The torque is calculated in cascade control. After that it acts on the torsion bar on the right side. On the left side there is the arm of the robot. Parameters of torsion bars correspond to the expected used

motor. We need two other coordinates for a rotation description of motor shaft. These two new coordinates are φ_1 and φ_2 as you can see it on *Picture 4* on right side.

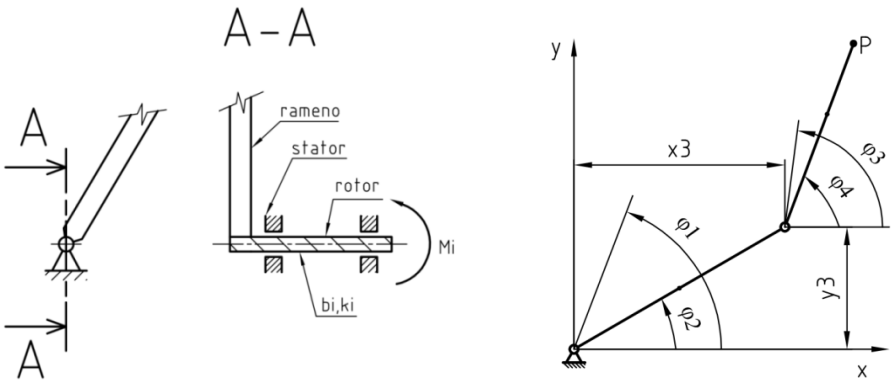

***Picture 4**- Drive submissiveness*

2.2 Cascade control

For all previous work we used the cascade control regulation. In the first phase, we observed the difference between the desired and actual position and the speed of the motor. You can see the second phase in *Picture 5*. We added the cascade for monitoring of the arm and motor rotation. At the end we chose a single cascade to monitor the difference between desired position and velocity directly from the actual rotation of the shoulder.

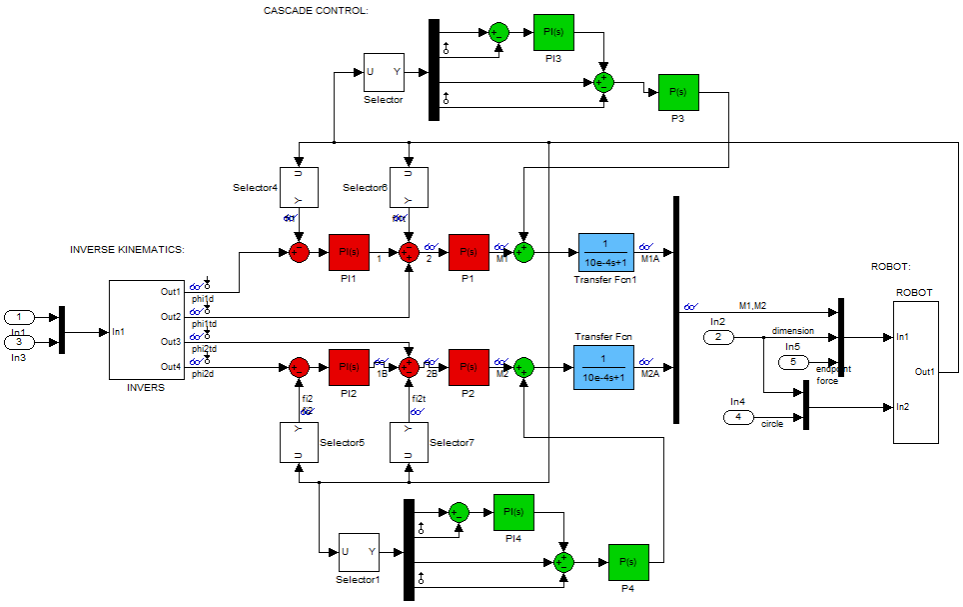

***Picture 5** - Two cascades*

2.3 Quality of the proposed mechanism

The quality of the proposed mechanism was evaluated according to the system stability, accuracy in tracking the desired trajectory and dynamic stiffness. We determined the stability from the response to the jump of load power on the ending gripper and jump of desired position of endpoint. We could read the accuracy directly from the graph of deviation. As a test trajectory, we choose a circle, which sufficiently effects the behavior in the whole

workspace. While watching the trajectory we loaded the endpoint with force perpendicular to the trajectory. According to the perpendicular direction it replaces machining of shaft or hole.

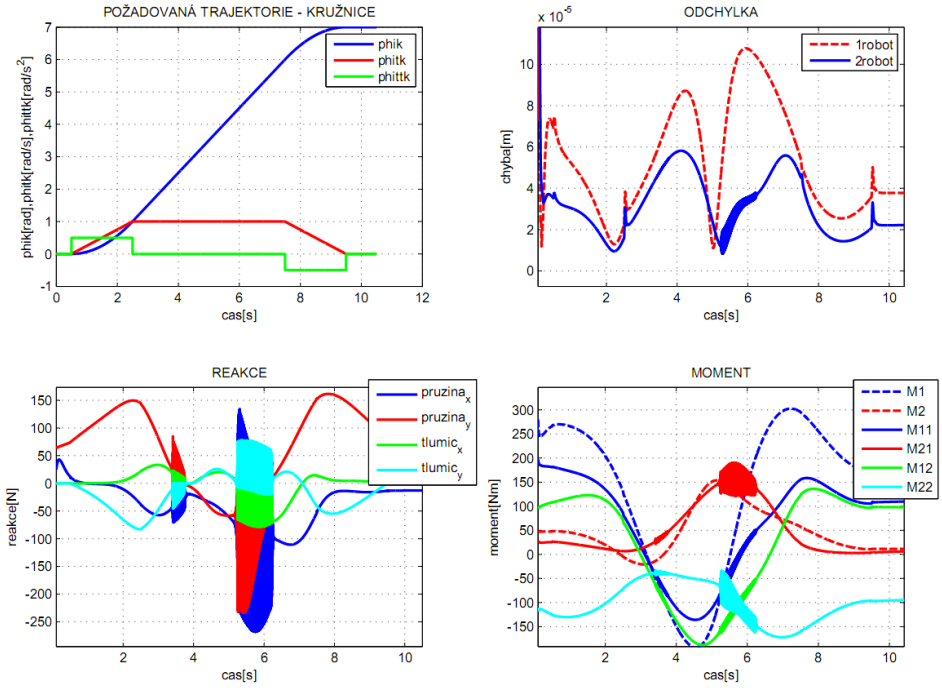

Picture 6 *– Graphs – two cascades*

As example on the *Picture 6* there are graphs from system testing with two cascades. Test mode is tracking in desired trajectory. Desired trajectory is circle. On top left there are desired parameters (position, velocity, acceleration). On top right there is deviation of endpoint position. Lower left there is reaction within the connenting element. Lower right there are torques. You can see that the connection of two robots with control by two cascades brings vibration.

2.4 Dynamic stiffness

One of the main parameters of the machine tool seems to be dynamic stiffness, which very well characterizes the quality of the designed machine. Its size tells us whether it is possible to use mechanism for machining and "how quickly and well" is this machining possible.
Source *[8]* states that the effect of solitary harmonic forces Fk on the grid induces harmonic motion for the coordinate *xj(t)* given by relationship

$$x_j(t) = \sum_{i=1}^{n} \frac{v_{ij} v_{ki}}{\lambda_i - \lambda} F_k \qquad (1)$$

Here λ_i are eigenvalues, v_{ij} are eigenvectors and $\lambda=\omega^2$. Sum is called dynamic submissiveness. The same relationship can also describe the expression

$$S_{xx} = |H|^2 S_{ff} \qquad (2)$$

Here S_{ff} is spectral power density of the signal of input power and S_{xx} is the spectral power density of endpoint displacement. The symbol H denotes the frequency response according to *[7]*. However, it also determines the dynamic submissiveness.

$$H(\omega) = \sqrt{\frac{S_{xx}(\omega)}{S_{ff}(\omega)}} \quad (3)$$

If the expression *(3)* describes the dynamic submissiveness, its inverse value represents the dynamic stiffness.
When determining the dynamic stiffness we start from evaluating the input power signal and signal of endpoint deflection change. Before the load application, the fixed displacement of system from the desired value is taken as zero. The load force will thus vary from zero to the desired pulse. We loaded the endpoint by a pulse. The pulse in the system causes the entire frequency spectrum of different amplitude. We have created a spectral power density of the measured signals of the deflection of the end point and the input power. Into equation *(3)* we gradually substituted values of the spectral power densities of the two signals for the same frequency. Thus we received transmission for dynamic submissiveness.

3. Improvment after the connection

When testing the system with all the above-described types of control, the results were two-times better after the connection. The fundamental difference, however, was the progressively increasing control accuracy, it was itself achieved by the robot. The last controlling, which focused directly on desired position, velocity deviation from the actual position, velocity of the arm in accuracy and dynamic stiffness of the system, has improved several times compared to the first system.

3.1 Workspace

We first tested the space defined by the above-described circle. In the following testing, we have focused on other accessible areas of the workspace. We found the area plotted in *Picture 7*, there have been improvements up to eightfold. On the top there is no vibration in this space.

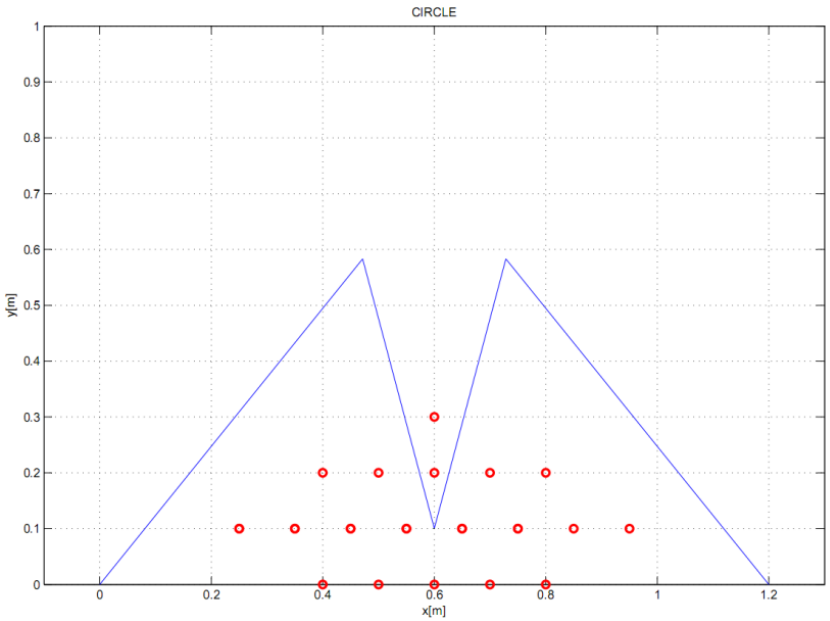

Picture 7 *- Space with a significant improvement*

3.2 Design-by-optimization

In the found space there we observed dragging, that is characteristic of redundantly driven parallel kinematics. That is why we joined the controlling *Design-by-optimization [3]*. As shown in the graph in *Picture 8* we terminated dragging.
If we set the ending gripper to different part of space than it is defined in *Picture 7*, there were significant vibration. In contrast to these points can be noted that the system was stable when prestressed connected.

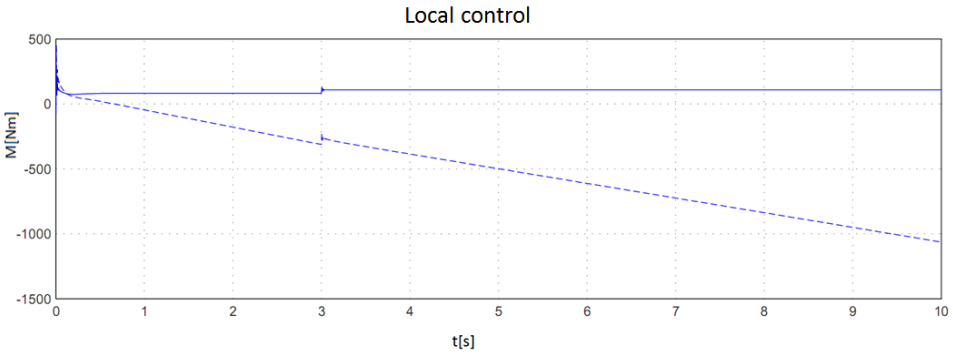

Picture 8 *– Torgue loads, Design-by-optimization*

4. Conclusion

The red line in the graph in *Picture 9* shows the behavior of the dynamic stiffness of the robot itself with one cascade observing the deviation from the desired motor rotation position. The blue line shows the system of connected robots with direct observing of arm rotation. As we can see, there is sometimes up to 25 times better result. This is all within an accuracy of 10^{-6} m.

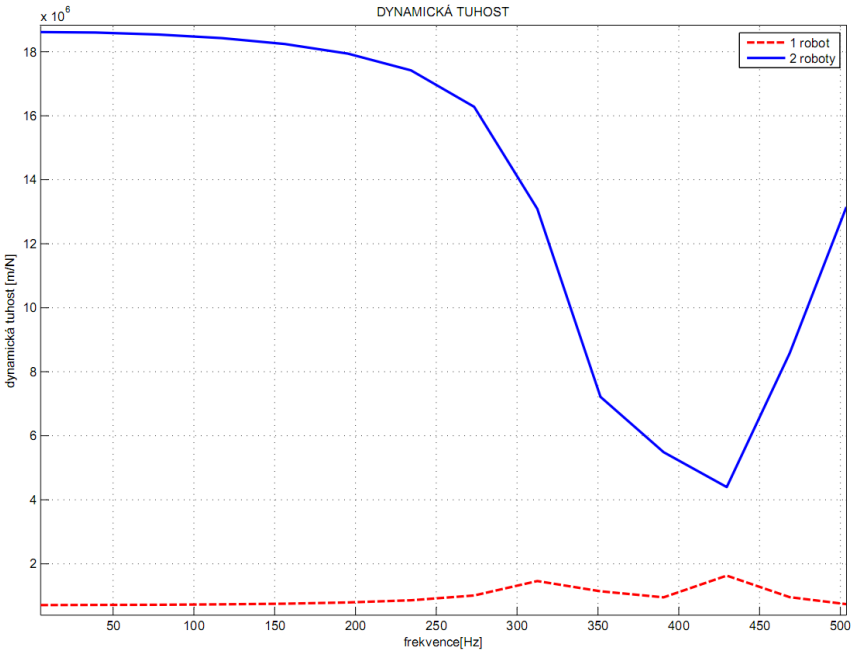

Picture 9 *– Torgue loads, Design-by-optimization*

Up to today the testing of simulated system showed that the mere combination makes only a twofold improvement. Multiple improvement has been found only in certain parts of the

working area. Further improvement was achieved only by introducing a different kind of controlling.
From the existing work there are some challenges for the further development and testing. The first task is to find the ideal configuration of cooperating robots in space. In the connection with previous we can also find dependences of observed parameters on the chosen configuration. The second task is to test the properties of cascade control observing directly rotary position of the arm, influence on the vibration etc. The final task is to test the system for different stiffness of the coupling element also included drives compliance.

List of symbols

m_1	Rotor 1 weight	$[kg]$
m_2	Arm 2 weight	$[kg]$
m_3	Rotor 3 weight	$[kg]$
m_4	Arm 4 weight	$[kg]$
m_s	Connecting element weight	$[kg]$
l_2	Arm 2 lenght	$[m]$
l_4	Arm 4 lenght	$[m]$
t_2	Center of gravity of arm 2	$[m]$
t_4	Center of gravity of arm 4	$[m]$
F	Force acting on the endpoint	$[N]$
S_{xx}	Spectral power density of endpoint displacement	$[W/Hz]$
S_{ff}	Spectral power density of the signal of input power	$[W/Hz]$
H	Frequency response (dynamic submissiveness)	$[N/m]$
x_j	Point coordinates	$[m]$
F_k	Harmonic force	$[N]$
v_{ij}	Eigen values	$[\ -\ ]$
λ_i	Eigenvectors	$[\ -\ ]$

References

[1] Valášek, M.: Mechatronika. Publishing CTU, Prague, 1996.
[2] Valášek, M.: Dynamic Time Parametrization of Manipulator Trajectories, Kybernetika 23(1987), 2, 154-174.
[3] Valášek, M. et al.: Design-by-Optimization and Control of Redundantly Actuated Parallel Kinematics Sliding Star, Multibody System Dynamic. 2005, vol. 14, no. 3-4, p. 251-267.
[4] Visual documentation of the product Trijoint 900H company Kovosvit MAS,a.s. Available from http://www.kovosvit.cz/trijoint/czech/cfoto.php
[5] Sliding Star vyroben FS ČVUT, Praha. Dostupné z http://mech.fsik.cvut.cz/doku.php?id=deptofmech&rev=1243950719
[6] Example of robot with linear kinematics, KR 1000 L950 TITAN P firmy KUKA Roboter GmbH. Available from http://www.kuka-robotics.com/czech_republic/cs/products/industrial_robots/special/palletizer_robots/kr1000_l950_titan_pa/start.htm
[7] Miláček, S.: Náhodné a chaotické jevy v mechanice, Publishing CTU, Prague, 2000.
[8] Brepta, R., Půst, L., Turek, F.: Mechanické kmitání, Sobotáles, Prague 1994.
[9] Spong, W., M.,: Underactuated Mechanical Systems, Coordinated Science Laboratory, University of Illinois at Urbana-Champaign, . Available from http://people.csail.mit.edu/katiebyl/ucsb/ece594d/papers/Spong97.pdf.